*Journal of Applied Mechanics and Technical Physics, Vol. 49, No. 3, pp. 484–490, 2008*

# PLASTIC MACRODEFORMATION OF POLYCRYSTALLINE AND SUBMICROCRYSTALLINE TITANIUM FOR BIOMEDICAL APPLICATIONS

**I. O. Bolotina,**[1] **V. I. Danilov,**[2] **and A. A. Zagumennyi**[2]

UDC 669.1'7882:539.374

*The deformation behavior of commercially pure submicrocrystalline and coarse-grained titanium was studied at the macroscopic level. Stress–strain curves of the materials were analyzed. Time–space distributions of local strains were studied at all stages of strain hardening using speckle interferometry. The life time of test specimens of the materials and the coordinates of the fracture region were calculated theoretically and confirmed experimentally. The motion of the zones of localized plasticity was studied. The prefracture stage was shown to involve "condensation" of the zones of localized plasticity and migration of deformation to the fracture neck.*

**Key words:** *plastic deformation, strain localization, submicrocrystalline and polycrystalline titanium, kinetics of zones of localized plasticity, fracture.*

**Introduction.** Metallic materials for medical applications must meet the following requirements: be biologically inert on exposure to aggressive media and withstand various long-term mechanical loads. It is known that the chemical elements whose atomic weight is greater than that of iron are harmful to the human organism [1]. The light metals widely used in engineering, for example, magnesium or aluminum, react vigorously with organic acids and, hence, are also unsuitable. From this point of view, titanium has a unique compatibility with organism tissues. Long-term clinical tests have shown that titanium is very suitable for use in implants and prostheses for bone and soft tissues: the structure of the tissues surrounding titanium have not changed for a long time [2]. However, an increased content of impurities, including alloying elements, considerably reduces the biocompatibility of titanium; therefore, titanium based surgical implants can be produced using only high-purity titanium.

We note that the main drawbacks of pure titanium are a low wear resistance, a small elastic modulus, and an insufficient fatigue resistance, which can result, for example, in a fracture of bone screws due to torque [1]. In engineering, these problems are solved by using titanium alloys, but, as noted above, this method is undesirable for medical materials technology.

The mechanical characteristics of pure titanium can be improved by producing a nanostructural (submicrocrystalline) state over the entire volume [3]. At present, bulk nanocrystalline materials are produced by methods of intense plastic deformation [3, 4]; therefore, accounting for the deformation behavior of ultrafine materials is of great significance in both the manufacture of articles from them and in predicting the service behavior of the articles.

In all cases, as is known, plastic deformation develops nonuniformly and is localized at the macrolevel, with the localization pattern and its evolution largely determined by characteristics such as the plasticity margin, service life, and type of fracture. Studies [5–7] using more than 20 types of single-crystalline and polycrystalline

[1]Tomsk Polytechnical University, Tomsk 634050; irina-bol@mail.ru. [2]Institute of Physics of Strength and Materials Science, Siberian Division, Russian Academy of Sciences, Tomsk 634021; dvi@ispms.tsc.ru; zaa@ispms.tsc.ru.
Translated from Prikladnaya Mekhanika i Tekhnicheskaya Fizika, Vol. 49, No. 3, pp. 164–172, May–June, 2008. Original article submitted March 20, 2007; revision submitted April 4, 2007.

 

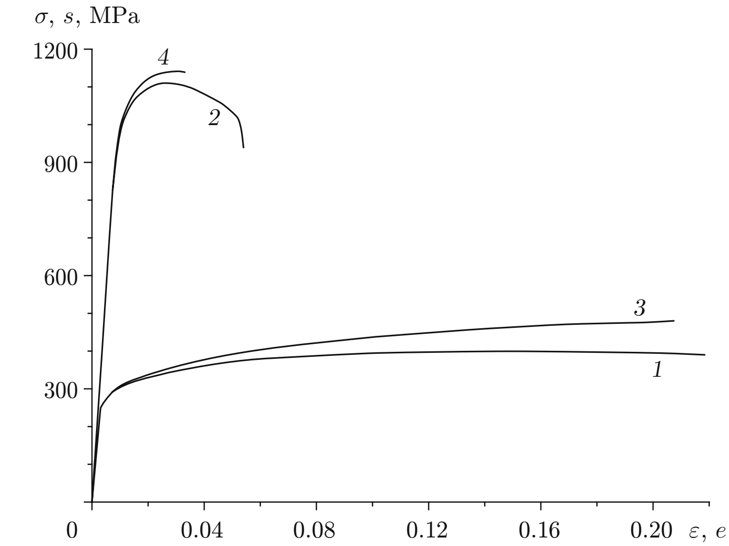


Fig. 1. Curves of $\sigma(\varepsilon)$ (1 and 2) and $s(e)$ (3 and 4) for titanium with coarse-grained structure (1 and 3) and submicrocrystalline structures (2 and 4).

materials, including metals, alloys, and nonmetals with various crystal structures and plastic flow micromechanisms have shown that the localization patterns and their evolution are determined by the nature of loading diagrams. Nanostructural materials have very unusual stress–strain curves and, hence, might be expected to exhibit unusual development of plastic flow localization.

**Structure and Strain Diagrams of the Materials Studied.** We studied commercially pure VT1-0 titanium containing 0.12% O, 0.18% Fe, 0.07% C, 0.04% N, and 0.01% H. The initial coarse-grained specimens of the double blade type with $1 \times 6 \times 40$ mm working section were machined from cold rolled sheets and annealed in argon at $T = 1023$ K for 1 h. In this state, their microstructure is represented by equiaxial grains of $\alpha$-Ti c with a characteristic size of 10–15 $\mu$m (submicrocrystalline specimens of this material were produced and certified at the Interdepartmental Laboratory of Biocompatible Implants and Coatings, Institute of Physics of Strength and Materials Sciences, Siberian Division, Russian Academy of Sciences).

The production of nanostructural titanium involved two steps. In the first stage, the titanium workpieces were subjected to multistage uniaxial compression in a closed mold at rates of $10^{-3}$–$10^{-2}$ sec$^{-1}$ and with a sequential stepwise temperature decrease from $T = 1023$ K to $T = 623$ K. Each cycle at a given temperature included three-stage or four-stage uniaxial compression with a change in the strain axis. In the second step, the titanium workpieces were subjected to plastic deformation by rolling in smooth rolls at room temperature. The total strain reached 90%. The strips produced by rolling were used to prepare tensile specimens, which had the same shape as the coarse-grained specimens. The specimens were subjected to precrystallization annealing in argon at $T = 523$ K for 1 h. Thus, commercially pure VT1-0 titanium had a homogeneous, equilibrium, and thermally stable (practically up to $T = 523$ K) granular-subgranular structure with a mean characteristic size smaller than 100 nm, which can be qualified as submicrocrystalline. Titanium with this structure has a high microhardness $H_\mu = 3200$ MPa, a high static strength $\sigma_{0.2} = 1000$ MPa and $\sigma_{\rm b} = 1100$ MPa, and satisfactory plasticity in uniaxial tension $\delta \geqslant 6\%$. (For comparison, for coarse-grained VT1-0 titanium, $H_\mu = 2800$ MPa, $\sigma_{0.2} = 270$ MPa, $\sigma_{\rm b} = 400$ MPa, and $\delta \geqslant 20\%$.)

The largest differences in mechanical behavior between submicrocrystalline and coarse-grained titanium were observed in an analysis of stress–strain curves (Fig. 1). In Fig. 1, it is evident that fracture of submicrocrystalline specimens occurs at higher tensions and three times smaller strains than fracture of coarse-grained titanium specimens (curves 2 and 1, respectively). It should also be noted that, after stress reached the ultimate value $\sigma_{\rm b}$ in the submicrocrystalline material, it decreases very slowly, so that a total strain is accumulated that exceeds the strain on the ascending portion of the curve: $\varepsilon_{\rm b} = 0.025$ and $\delta - \varepsilon_{\rm b} = 0.036$.

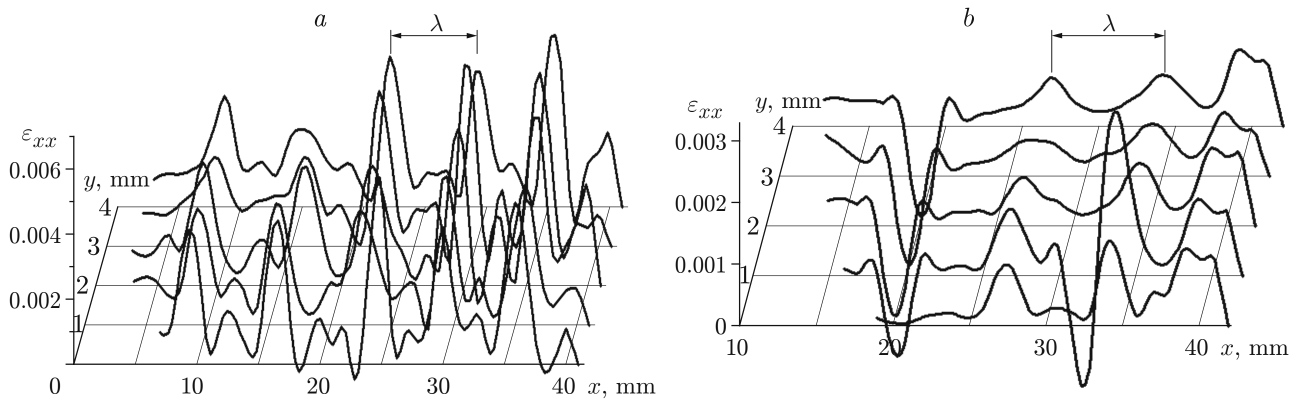


Fig. 2. Distribution of local elongations in deformed specimens in the Taylor stage for coarse-grained titanium (a) and submicrocrystalline titanium (b).

In coarse-grained and submicrocrystalline titanium, plastic flow have different sets of stages. An analysis of the stages was performed by logarithmation [6]. To identify stages, we used the value of the strain-hardening index $n$ included in the Taylor equation [8] for approximating strain curves of the general type:

$$s = s_0 + Ke^n. \tag{1}$$

Here $s$ is the true stress, $s_0$ is the critical stress at the onset of plastic flow, $K$ is the parabolic strain-hardening coefficient, $e$ is the true (logarithmic) strain. In this case, the portion of the strain curve with $n = 1$ corresponds to linear hardening, the portion with $n \approx 0.5$ to parabolic Taylor hardening, and the portion with $n < 0.5$ to prefracture [6, 7, 9].

An analysis of the stages of the stress–strain curve of coarse-grained titanium shows that the ascending portion of the curve corresponds to a short stage of linear hardening at $0.008 \leqslant \varepsilon \leqslant 0.014$, a stage of Taylor hardening with a strain-hardening index $n = 0.56$ at $0.019 \leqslant \varepsilon \leqslant 0.041$, and a stage with $n \approx 0.4$ at $0.075 \leqslant \varepsilon \leqslant 0.160$. It is evident that the deformation stages are divided by portions on which the hardening indices vary irregularly. The loading curve of submicrocrystalline titanium does not have a stage of linear hardening. A stage of Taylor hardening with $n \approx 0.5$ corresponds to a considerable part of the ascending branch ($0.010 \leqslant \varepsilon \leqslant 0.024$), which is followed by a portion on which hardening is almost absent ($n = 0.06$ and $0.025 \leqslant \varepsilon \leqslant 0.040$). In the conditional stresses and strains, this portion is on the descending branch.

**Analysis of Localized Plastic Deformation Patterns of Coarse-Grained and Submicrocrystalline Titanium.** Local-strain distributions were recorded using two-exposition speckle photography (see, for example, [10]). This method provides time–space distributions of the local components of the distortion tensor of the specimen being deformed. Figure 2 shows spatial distributions of the local elongations $\varepsilon_{xx}$ at the Taylor stages of the loading diagrams of coarse-grained and submicrocrystalline titanium. These distributions are sets of periodically located localization zones [5, 7]. In Fig. 2, it is evident that the distributions are qualitatively identical and differ only in the value of the spatial period $\lambda$ [$\lambda = (10 \pm 2)$ mm for submicrocrystalline titanium and $\lambda = (5 \pm 2)$ mm for coarse-grained titanium].

In the stage of linear hardening in the coarse-grained specimen, the local-strain distribution shows not only spatial periodicity but also time periodicity (Fig. 3). From Fig. 3, one can see that the position of the localization zones depends on the deformation time and that the localization zones move at identical constant velocities $v_{\rm aw} = 5 \cdot 10^{-5}$ m/sec, forming an autowave, described, for example, in [5].

In the stage of parabolic strain hardening (Taylor stage) with a hardening index of $n \approx 0.5$ in both coarse-grained and submicrocrystalline titanium, the distribution of local elongations is stationary (Fig. 4a and c), i.e., during the entire stage, the localization zones remain stationary and the strain amplitudes in them are almost identical. Only by the end of this stage in submicrocrystalline titanium does the strain amplitude increase in the zone with the coordinate $X_s = 38.5$ mm.

In the prefracture stage in both coarse-grained and submicrocrystalline titanium, the kinetics of the localized deformation zone changes significantly again: all localization zones, except for one, start moving (Fig. 4b and c). In

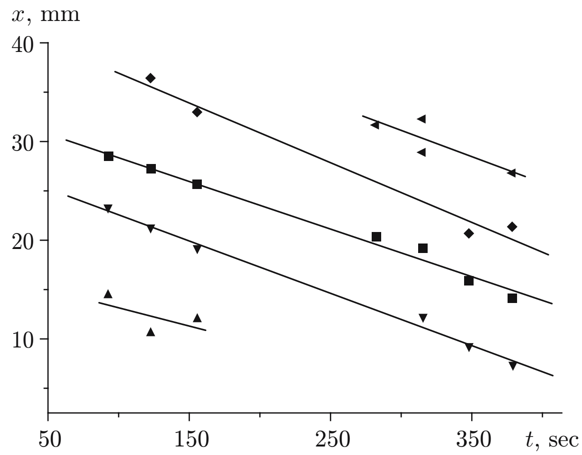


Fig. 3. Kinetics of the zones of localized plastic deformation in the linear stage in coarse-grained titanium.

coarse titanium, this zone has the coordinates $X_s = 7.5$ mm, and in submicrocrystalline titanium, $X_s = 38.5$ mm. For both materials at the prefracture stage, the diagrams of motion of the deformation zone are bundles of lines converging to the focal point $(X_s, t_{\rm f})$ ($t_{\rm f}$ is the time of deformation to fracture). Fracture of the specimens occurs in the stationary localization zone [6, 9].

It is known that displacement diagrams of any objects form a bundle of straight lines provided that their velocities depend linearly on the initial coordinates, i.e., the following condition is satisfied [11]:

$$V(X_0) = \alpha X_0 + \beta.$$

Here $X_0$ are the initial coordinates of the objects and $\alpha$ and $\beta$ are constants. In the case considered, the velocities of motion of the localized-plasticity zones and their corresponding initial coordinates are determined experimentally from the slope of the straight lines in Fig. 4b and c. It is evident from Fig. 5 that the dependence $V(X_0)$ is linear for both submicrocrystalline and coarse-grained titanium.

For the self-consistent motion of the localization zones at the prefracture stage, we have

$$\alpha = 1/t_{\rm pf}, \qquad \beta = -X_{\rm f}/t_{\rm pf}$$

($t_{\rm pf} = t_{\rm f} - t_0$ is the duration of the prefracture stage; $X_{\rm f}$ is the coordinate of the fracture site; $t_0$ is the time of deformation before the onset of this stage). Consequently, the life time of a specimen and the coordinate of the fracture site can be estimated from the constants $\alpha$ and $\beta$ determined by the approximating straight lines (Fig. 5). For submicrocrystalline titanium, $X_{\rm f} = 40.5$ mm and $t_{\rm f} = 615$ sec, and for coarse-grained titanium, $X_{\rm f} = 6$ mm and $t_{\rm f} = 2080$ sec. These values are in reasonable agreement with experimental values. The submicrocrystalline specimen fractured in 630 sec after the beginning of deformation at 39 mm from the stationary testing-machine head, and the coarse-grained specimen in 2150 sec at 7.5 mm from it.

In [9], the nature of motion of localized plastic deformation domains and the dependence of their velocities on the coordinates of these domains are attributed to a change in the deformation properties of some macroscopic volumes of the material in the prefracture stage. In [5, 7], it is shown that, in the linear hardening stage [$n = 1$ and $ds/de = nKe^{n-1} = \theta = \text{const}$, according to (1)] the velocity of the localized plasticity fronts is constant and inversely proportional to $\theta$. In the Taylor stage ($n = 0.5$), the localization zones are stationary. In the remaining cases ($n \neq 0.5$), the velocity of the localized plastic deformation zones obey the relation [7, 12]

$$V(n) = V_0(n - q)^2 \tag{2}$$

($V_0$ is an empirical constant and $q \approx 0.5$). Therefore, any difference in the velocities of the localized plastic deformation zones is due to local changes in the strain hardening characteristics $n$ and $K$ [see (1)]. In [7, 9], by normalizing expression (2) to experimental velocities corresponding to the linear-hardening stage ($V_{\rm II} = \text{const}$ and $n \approx 1$) and the Taylor stage ($V_{\rm III} = 0$ and $n \approx 0.5$), the values of $V_0$ were determined for a number of materials and the indices $n$ were estimated for each moving zone of localized plastic deformation in the prefracture stage. In the

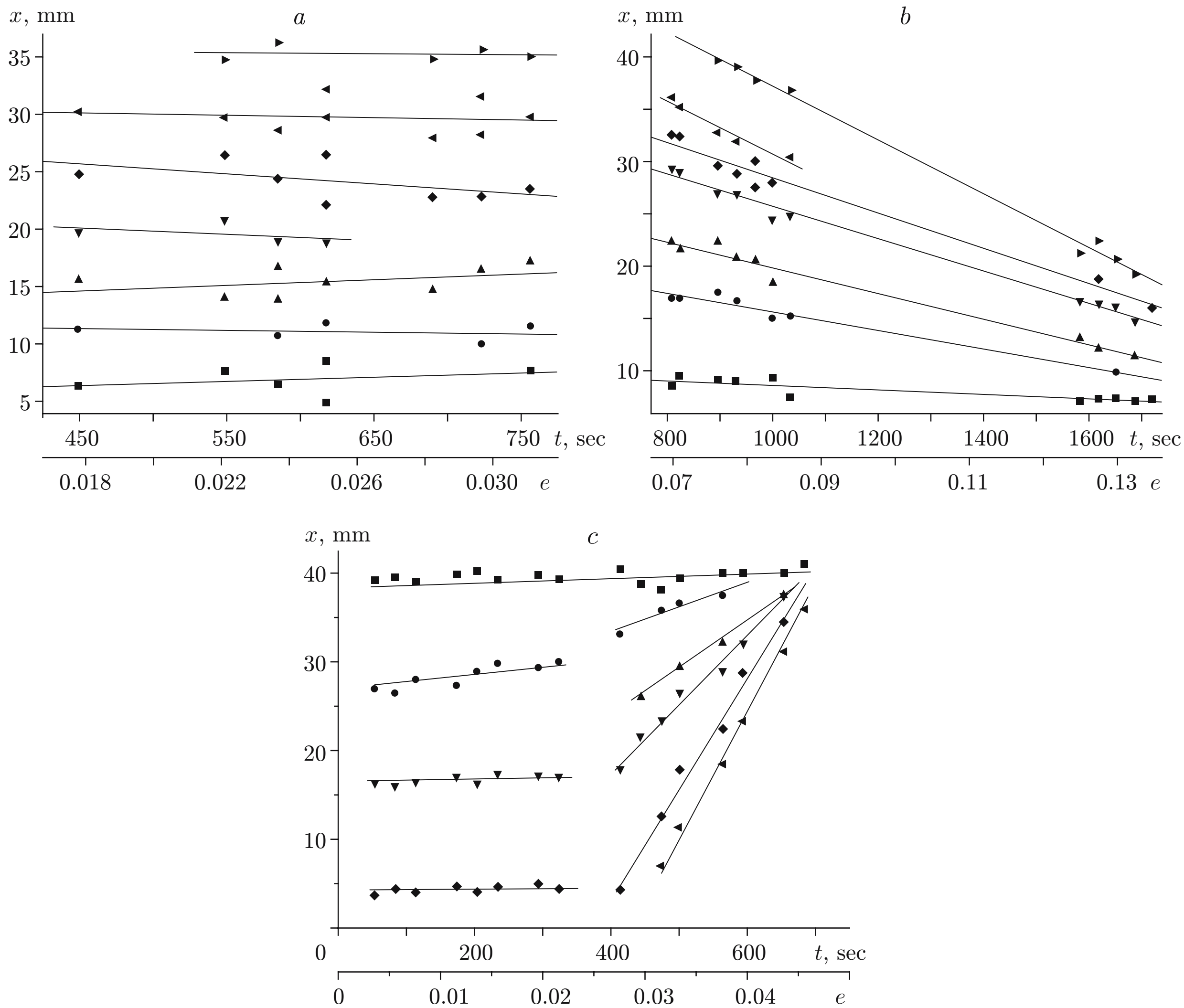


Fig. 4. Kinetics of the zones of localized plastic deformation of coarse-grained titanium in the Taylor stage (a) and prefracture stage (b), and during tension of submicrocrystalline titanium (c).

present study, this was done for coarse-grained titanium (in submicrocrystalline titanium, $V_0$ cannot be determined since a linear hardening stage is absent). The calculation results are presented in Fig. 6. It is evident that the dependence $V(n)$ is parabolic. The largest value of the hardening index corresponds to the stationary localization zone, and for the remaining domains, its value is much smaller than the average value throughout the prefracture stage, which is equal to 0.4.

Thus, in the prefracture stage, the active zone of plastic deformation decreases and, in the remaining part of the specimen, the plastic flow decays. There is "condensation" of the zones of localized plastic deformation and migration of deformation to the fracture neck.

In some materials in the prefracture stage, rapidly moving domains were found for $n < 0$ [9, 13]. It is known that this condition corresponds to the descending branch of the conditional stress–strain curve but the parabolic index determined for the specimen as a whole remains positive. This implies that, in plastic flow in the prefracture stage, both softening and hardening zones of localized plastic deformation can exist. It should be noted that localized plastic deformation domains with such deformation properties originate even in the prefracture stage. During deformation of coarse-grained titanium, all localization zones observed at the prefracture stage were formed even at the Taylor stage; this may be the reason why softening domains were not detected there.

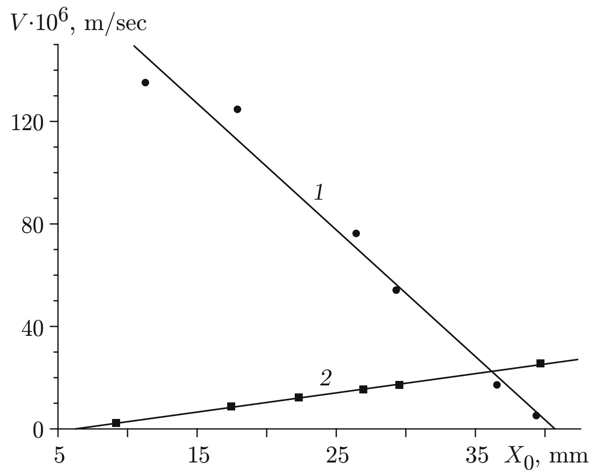


Fig. 5. Curves $V(X_0)$ for submicrocrystalline titanium (1) and coarse-grained titanium (2).

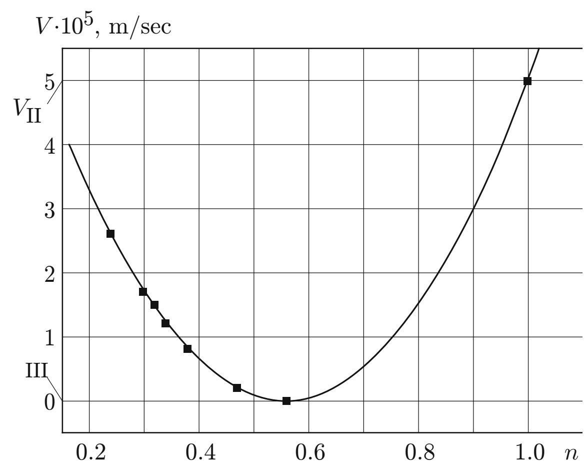


Fig. 6. Curve of $V(n)$ for coarse-grained titanium.

**Conclusions**. From the analysis of the stress–strain curves, it follows that in submicrocrystalline titanium specimens, fracture occurs at higher stresses and smaller strains than in coarse-grained titanium. The main difference is that, in submicrocrystalline titanium, after the stress reaches the ultimate values $\sigma_{\mathrm{b}}$, it decreases very slowly, resulting in the accumulation of the total strain exceeding the strain on the ascending branch of the curve. This means that local and global instabilities of the plastic flow occur simultaneously. In the coarse-grained material, a zone of future fracture becomes apparent even prior to the beginning of formation of a macroscopic neck, i.e., a local loss of stability occurs early enough, whereas, at the global level, quasi-homogeneous deformation of the material continues.

In the stage of parabolic hardening and prefracture, coarse-grained and submicrocrystalline titanium exhibit qualitatively similar deformation behavior. The algorithm for estimating the coordinates and time of future fracture proposed in the paper is in good agreement with experimental data.

It was shown that any difference in the velocity of localized plastic deformation domains is due to a local change in the strain-hardening characteristics $n$ and $K$. At the prefracture stage, the active zone of plastic deformation decreases and, in the remaining part of the specimen volume, the plastic flow decays. There is "condensation" of the localized plastic deformation zones and migration of deformation to the fracture neck. At this time, the localized plastic deformation domains evolve separately, so that the coexistence of hardening and softening regions of the material is possible.

Submicrocrystalline titanium has a high absolute value of the yield strength, and the difference between the yield strength and ultimate fracture strength is 10%. Due to these properties, structural materials, in particular, medical implants, can be used under elastic deformation conditions at constant temperatures. At the same time, the fact that, with a global loss of stability, submicrocrystalline titanium has considerable plasticity is of interest for technological purposes. In this case, distortion proceeds without hardening in a stable macroscopic deformation zone. Such conditions are produced in the production of members and structures by drawing, extrusion or rolling. Because these operations do not affect the submicrocrystalline state of the material, the products have the required performance.

We thank Yu. P. Sharkeev and A. Yu. Eroshenko for providing certified specimens of submicrocrystalline titanium.

This work was supported by the Russian Foundation for Basic Research (Grant No. 05-08-18248a) and Program of the President of the Russian Federation on the State Support of Leading Scientific Schools (Grant No. MK-5223.2006.8).

## REFERENCES

1. S. P. Vikhrov, T. A. Kholomina, P. I. Begun, and P. N. Afonin, *Biomedical Materials Technology*, Goryachya Liniya–Telecom, Moscow (2006).
2. A. V. Karlov and V. P. Shakhov, *Systems of External Fixation and Regulatory Mechanisms of Optimal Biomechanics* [in Russian], Izd. Sib. Gos. Med. Univ., Tomsk (2001).
3. R. Z. Valiev and I. V. Aleksandrov, *Nanostructural Materials Produced by Intense Plastic Deformation* [in Russian], Logos, Moscow (2000).
4. Yu. P. Sharkeev, A. D. Bratchikov, Yu. R. Kolobov, et al., "Nanostructural titanium for biomedical applications," *Fiz. Mezomekh.*, **7**, Special issue, 107–110 (2004).
5. L. B. Zuev, V. I. Danilov, and B. S. Semukhin, "Time–space hardening in plastic deformation of solids," *Usp. Fiz. Nauk*, **3**, No. 3, 237–304 (2002).
6. V. I. Danilov, L. B. Zuev, E. V. Letakhova, et al., "Types of localization of plastic deformation and stage of loading diagrams of metallic materials with different crystalline structures," *J. Appl. Mech. Tech. Phys.*, **47**, No. 2, 298–305 (2006).
7. L. B. Zuev, "On the waves of plastic flow localization in pure metals and alloys," *Ann. Phys.*, **16**, No. 4, 286–310 (2007).
8. R. W. K. Honeycombe, *The Plastic Deformation of Metals*, Edward Arnold, London (1984).
9. L. B. Zuev and V. I. Danilov, "On the kinetics of macrodomains of localized plasticity in the metal prefracture stage," *Zh. Tekh. Fiz.*, **75**, No. 12, 102–105 (2005).
10. V. I. Danilov, L. B. Zuev, V. V. Gorbatenko, et al., "Using speckle interferometry to study the localization of plastic deformation," *Zavod. Lab.*, **72**, No. 12, 40–45 (2006).
11. Ya. B. Zel'dovich and A. D. Myshkis, *Elements of Mathematical Physics* [in Russian], Nauka, Moscow (1973).
12. T. M. Poletika, G. N. Narimanova, S. V. Kolosov, and L. B. Zuev, "Plastic flow localization in commercial zirconium alloys," *J. Appl. Mech. Tech. Phys.*, **44**, No. 2, 262–270 (2003).
13. A. V. Strel'nikova, L. B. Zuev, and V. I. Danilov, "Localized plasticity ineformation and fracture of Duralumin," *Fiz. Mezomekh.*, **9**, Special issue, 87–90 (2006).